Physicochemical and Structural Characterization of Mesoporous Aluminosilicates Synthesized from Leached Saponite with Additional Aluminum Incorporation

Thierry Linssen,*,† Kristof Cassiers,† Pegie Cool,† Oleg Lebedev,‡ Andrew Whittaker,§ and Etienne F. Vansant†

Laboratory of Adsorption and Catalysis, Department of Chemistry, University of Antwerp (UIA), Universiteitsplein 1, B-2610 Wilrijk, Belgium, Centre for Electron Microscopy and Materials Science, University of Antwerp (RUCA), Groenenborgerlaan 171, B-2020 Antwerp, Belgium, and Centre for High Performance Polymers, University of Queensland, QLD 4072, Australia

Received August 5, 2003. Revised Manuscript Received October 2, 2003

A thorough investigation was performed on the physical (mechanical, thermal, and hydrothermal stability) and chemical (ion exchange capacity and silanol number) characteristics of aluminosilicate FSMs, synthesized via a new successful short-time synthesis route using leached saponite and a low concentration of CTAB. Moreover, the influence of an additional Al incorporation, utilizing different aluminum sources, on the structure of the FSM derived from saponite is studied. A mesoporous aluminosilicate with a low Si/Al ratio of 12.8 is synthesized, and still has a very large surface area of 1130 m^2/g and pore volume of 0.92 cm^3/g. The aluminum-containing samples all have a high cation exchange capacity of around 1 mmol/g while they still have a silanol number of about 0.9 OH/nm^2; both characteristics being interesting for high-yield postsynthesis modification reactions. Finally, a study is performed on the transformation of the aluminosilicates into their Brønsted acid form via the exchange with ammonium ions and a consecutive heat treatment.

Introduction

Hexagonal mesoporous materials (HMMs) such as folded sheet materials (FSM) have well-ordered hexagonal arrays of uniform one-dimensional pores with diameters from 15 to 300 Å and have attracted increasing attention as a support for preparing heterogeneous catalysts. In 1990 Yanigasawa et al.[1] proposed a pillaring method consisting of interlayer cross-linking of a single-sheet silicate kanemite ($NaHSi_2O_5 \cdot 3H_2O$) in an ion exchange reaction with organic cations. By calcinatio, the silicate−organic complexes were converted to mesoporous materials with uniform pore size distributions. This synthesis method was modified by Inagaki et al.[2] in 1993 to produce mesoporous materials called folded sheet materials (FSM) caused by its formation mechanism. They reported the formation of a long-ranged hexagonally ordered material by an electrostatic quaternary ammonium directed rearrangement (folding) of the single-sheet silicate kanemite. However, nowadays the mechanism is thought to be different. A hexagonal structure is created by condensation of silicate, which consists of derivatives of kanemite sheets, through the formation of a mosaic of hexagonal domains.[3]

The purely siliceous mesoporous materials have a chemically inert silicate framework and consequently no acid sites. Therefore, a large number of papers have appeared dealing with the incorporation of aluminum into the frameworks of HMMs.[4−7] Moreover, studies on the synthesis of mesoporous FSM aluminosilicates, with presumably improved physical and chemical properties, starting from layered silicates containing aluminum are also known in the literature.[8,9] Very recently, for the first time, we reported on the synthesis of FSM containing framework aluminum from leached natural saponite in order to obtain mesoporous materials with acidic surface properties in a short synthesis time (3 days instead of 15 days for the FSM synthesized from kanemite) and low surfactant concentration (3 wt % instead of 26 wt % for the MCM-41 synthesis).[10] These aluminosilicate mesoporous materials have high crystallinity, pore volume, and specific surface area, creating important potential opportunities for their use as heterogeneous acid catalysts.

* To whom correspondence should be addressed. E-mail: thierry.linssen@ua.ac.be. Phone: 0032(3)820.23.54. Fax: 0032(3)-820.23.74.
† Laboratory of Adsorption and Catalysis, UIA.
‡ Centre for Electron Microscopy and Materials Science, RUCA.
§ University of Queensland.

(1) Yanagisawa, T. *B. Chem. Soc. Jpn.* **1990**, *63*, 988.
(2) Inagaki, S.; Fukushima, Y.; Kuroda, K. *J. Chem. Soc., Chem. Commun.* **1993**, 680.
(3) O'Brien, S.; Francis, R. J.; Price, S. J.; O'Hare, D.; Clark, S. M.; Okazaki, N.; Kuroda, K. *J. Chem. Soc., Chem. Commun.* **1995**, 2423.
(4) Mokaya, R. *J. Chem. Soc., Chem. Comm.* **2000**, 1891.
(5) Corma, A.; Fornés, V.; Navarro, M. T.; Pérez-Pariente, J. *J. Catal.* **1994**, *148*, 569.
(6) Kosslick, H.; Lischke, G.; Parlitz, B.; Storek, W.; Fricke, R. *Appl. Catal. A* **1999**, *184*, 49.
(7) Reddy, K. M.; Song, C. *Catal. Lett.* **1996**, *36*, 103.
(8) Inagaki, S.; Yamada, Y.; Fukushima, Y. *Stud. Surf. Sci. Catal.* **1997**, *105*, 109.
(9) Kan, Q.; Fornés, V.; Rey, F.; Corma, A. *J. Mater. Chem.* **2000**, *10*, 993.
(10) Linssen, T.; Cool, P.; Baroudi, M.; Cassiers, K.; Vansant, E. F.; Lebedev, O.; Van Landuyt, J. *J. Phys. Chem. B* **2002**, *106*, 4470.

10.1021/cm031111a CCC: $25.00
Published on Web 11/20/2003

In the current literature, there are few reports on the synthesis route starting from leached clays, although it is highly possible to obtain materials with remarkably different surface chemistry by this route. The starting clays and extent of acid leaching can affect the solid characteristics, such as the surface properties. Therefore, the physical (mechanical, thermal, and hydrothermal stability) and chemical (ion exchange capacity and silanol number) features of these mesoporous aluminosilicates are thoroughly investigated in this paper. Second, the influence of an additional Al incorporation, utilizing different aluminum sources, on the structure of the FSM derived from saponite was studied. The acidic properties of these new materials were also investigated in detail and will be published soon.

Experimental Section

(a) Materials. Saponite from near Ballarat, CA, supplied by the Source Clay Repository of the Clay Minerals Society, is used in this work. The clay contains up to 3% diopside and tremolite, separable by wet sedimentation. Saponite, a natural trioctahedral clay with a TOT-structure has an octahedral layer consisting of mainly $Mg(O, OH)_6$-octaheders condensed between two tetrahedral layers consisting of mainly $Si(O, OH)_4$-tetraheders. Sodium ions are located in the interlayer region to compensate for the negative charge on the sheets. The idealized chemical formula is $Na_{0.32}Ca_{0.38}(Si_{7.54}Al_{0.76})Mg_{5.22}O_{20}(OH)_4$. The exchangeable ions provide the untreated saponite a cation-exchange capacity (CEC) of 1.04 mmol/g. The size of the clay platelets used is $<2\ \mu$m in diameter and 9.6 Å in height.

For the incorporation of aluminum into the structure three aluminum sources were used being, sodiumaluminate or $NaAlO_2$ (Riedel-de Haën, anhydrous, technical), aluminumnitrate or $Al(NO_3)_3$ (Fluka Chemika, 98.0%), and aluminum triisopropoxide or $Al(i\text{-}C_3H_7O)_3$ (Fluka Chemika, 99%).

Quantification of the silanol number was performed via the reaction of the isolated silanols with trimethylchlorosilane or TMSCl (Merck, +99%) in the presence of a catalysator being triethylamine or Et_3N (Merck, +99%).

Investigating the ion exchange capacity of the samples, ammonium nitrate (Merck, +99%) was used as a source for the exchanged ammonium ions.

(b) Sample Preparation. A 2.5-g sample of the natural saponite was leached under stirring at 25 °C for 24 h by 20 mL of 8 M HCl aqueous solutions to remove the magnesium-containing octahedral layer. The leached silicate powders were washed and filtered several times to remove all HCl.

The aluminosilicate FSM precursors were prepared according to the method described before.[10] The leached saponite was suspended in 20 mL of solution using 0.1 M cetyltrimethylammonium bromide (CTAB) as structure directing agent and 1 g of the dried leached silicate powders as silicate source, and denoted correspondingly as FSMSap. The suspension was adjusted to a pH of 12.3 with 2 M NaOH and stirred for 3 h at 70 °C. After 3 h the solid was filtered and dispersed in 20 mL of distilled water, and the pH of the dispersion was adjusted to 8.5 with 2 M HCl. This suspension was stirred for a subsequent 3 h at room temperature. Additional incorporation with different aluminum sources was performed by adding 0.02 g of $NaAlO_2$, 0.09 g of $Al(NO_3)_3 \cdot 9H_2O$, or 0.05 g of $Al(i\text{-}C_3H_7O)_3$ together with the leached saponite during the first step of the synthesis; the obtained samples are referred to as FSMSap $Al(NO_3)_3$, FSMSap $NaAlO_2$, and FSMSap $Al(i\text{-}C_3H_7O)_3$, respectively. The expected Si/Al ratio if the aluminum would be fully incorporated is in all cases 8. All the samples were calcined at 550 °C for 6 h in air with a heating rate of 2 °C/min to obtain the mesoporous structure (Figure 1).

Subsequently, the resulting Al−FSMSaps are converted into their acid form by extracting the Na^+ form 3 times for 2 h with a pure 0.5 M NH_4NO_3 solution using a liquid-to-solid ratio of 20 wt %. The NH_4^+ form was then calcined a second time at 550 °C for 6 h to obtain the acid form during the desorption of NH_3.

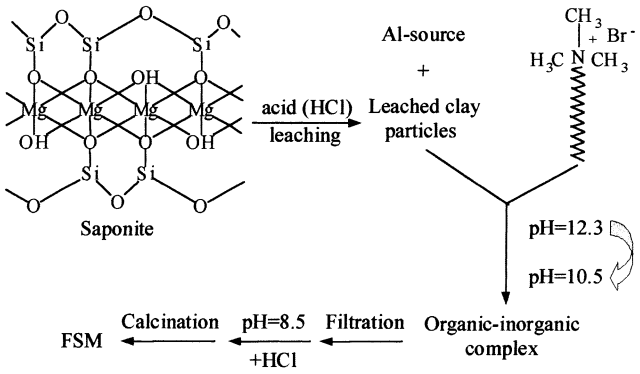

Figure 1. Procedure to synthesize FSM with different Al sources starting from leached saponite.

To compare the eventual FSMSaps with a standard, the original FSM synthesized from kanemite was calcined according to Inagaki's method.[2]

(c) Characterization Methods. The chemical compositions of the FSMSap samples in the Na^+ form and the acid form were determined by electron probe micro analysis (EPMA) using a JEOL JCX electron microprobe analyzer. The obtained samples were stored in a nitrogen glovebox to avoid hydration until examination of their structure by X-ray powder diffraction (XRD) and N_2 adsorption. The XRD patterns were measured on a Philips PW 1840 powder diffractometer with Cu Kα radiation ($\lambda = 1.540$ Å), 45 kV, 30 mA, and a Ni filter. Nitrogen adsorption−desorption isotherms of the calcined FSM materials were recorded at 77 K on a Quantachrome Autosorb-MP automated gas adsorption system. The samples were degassed at 150 °C during 16 h in a vacuum furnace prior to analysis. Surface areas were calculated according to the BET equation, whereas the total pore volumes were calculated from the adsorbed amount at a relative pressure $p/p_0 = 0.98$. Pore size distributions were obtained from the adsorption branch following the method of Barrett, Joyner, and Halenda (BJH). TEM investigations were carried out with a JEOL 4000EX microscope operated at 400 kV to analyze the structure of the FSMSap. The point resolution of the microscope was of the order of 0.17 nm.

(d) Physical Properties. *Mechanical Stability*. Mechanical tests were performed by pelletizing each powder into a die with a diameter of 13 mm. The pressure was increased in steps of 74 MPa and was kept constant for 2 min.

Thermal Stability. To assess thermal stability, all samples were calcined in air starting from an end temperature of 550 °C. The end temperature was increased in steps of 100 °C as long as no complete collapse of the mesostructure occurred. All of the sample precursors were calcined at a heating rate of 2 °C/min and kept at the end temperature for 6 h.

Hydrothermal Stability. The hydrothermal stability study was conducted by exposing the samples to a nitrogen stream containing a 30 vol % of water vapor at 400 °C for 48 and 120 h. The flow of the N_2 stream was kept at 100 mL/min with a pressure of 1 atm. In addition, all samples were also exposed to steam in a more severe test at 100 °C for 16 h at autogenous pressure with a relative humidity of 100%.

(e) ^{27}Al MAS NMR. ^{27}Al NMR high-speed magic angle spinning (MAS) spectra of the powdered samples were recorded applying a MAS spinning speed of ca. 7−8 kHz on a MSL300 spectrometer ($B_0 = 7$ T). The estimated values of the chemical shift for differently coordinated Al sites are derived from signal deconvolution. Data were not corrected for second-order quadrupole effects. To get the best fit of the Al NMR spectra, the Gauss−Lorentz ratios and the line widths of the individual signals were varied. Despite the known uncertainties caused by quadrupole coupling effects on signal intensities,

Table 1. Physicochemical Properties of the FSMSap Samples in the Na^+ and H^+ Form

sample	Si/Al ratio	*a* (nm)	N_2 adsorption data S_{BET} (m^2/g)	PV (cc/g)	∅ (nm)	CEC_{max} (mmol/g)	CEC (mmol/g)	n_{OH} (OH/nm^2)
				Na^+ Form				
FSMSap	12.8	4.5	1130	0.92	2.7	1.0	1.1	
FSMSap $NaAlO_2$	10.6	5.0	565	0.98	3.0	1.2	1.1	
FSMSap $Al(NO_3)_3$	10.7	4.6	399	0.42	3.1	1.1	1.0	
FSMSap $Al(i\text{-}C_3H_7O)_3$	12.4	4.6	426	0.43	3.1	1.1	1.0	
				H^+ Form				
FSMSap	13.2	4.5	254	0.16	2.5			0.8
FSMSap $NaAlO_2$	11.0	5.0	405	0.33	3.2			0.6
FSMSap $Al(NO_3)_3$	11.3	4.8	348	0.31	3.1			0.6
FSMSap $Al(i\text{-}C_3H_7O)_3$	11.4	4.6	441	0.32	2.9			0.7

and the general problems connected to the deconvolution of strongly superimposed spectra, the relative portions of the differently coordinated Al species are reflected.

(f) Determination of the Cation Exchange Capacity. The samples in the sodium form were stirred three subsequent times for 2 h in a pure 0.5 M NH_4NO_3 solution using a liquid-to-solid ratio of 20 wt %. Via determination of the nitrogen content of the samples with the Kjeldahl method after exchange of the sodium ions with ammonium ions, the actual cation exchange capacity (CEC) was calculated.

(g) Quantification of the Silanol Number. To determine the silanol number (OH/nm^2) the isolated surface silanols were allowed to react under a nitrogen atmosphere with TMSCl in the presence of a catalyst (Et_3N) in a 1:1 ratio. Therefore, to avoid hydration of the isolated silanols, the samples were transported directly after calcination at 550 °C to the reaction mixture consisting of TMSCl and Et_3N dissolved in CH_2Cl_2 under a N_2 flow. The amount of TMSCl, reacted for 2 h in a 1:1 ratio with the isolated silanols, was determined with thermogravimetric analysis (TGA) measuring the weight loss caused by the oxidation of the organics at 500 °C. TGA was performed on a Mettler TG 50/TA 3000 thermobalance controlled by a TC10A microprocessor. The samples were heated at a rate of 10 °C/min under an O_2 flow of 150 mL/min.

The organics being oxidized at 500 °C were investigated with infrared measurements. The in situ DRIFT measurements were performed on a Nicolet Nexus 670 bench equipped with an in situ Spectra Tech high-temperature vacuum chamber, controlled by a Spectra Tech time-proportional temperature controller and a MCT detector. Samples were mixed with KBr (95% KBr, 5% sample). Spectra were collected in air at various temperatures starting from room temperature up to 500 °C. The resolution of the spectrum is 4 cm^{-1}.

Carbon microanalyses were carried out in a Perkin-Elmer CHN analyzer to verify the reliability of the TGA measurements toward the quantification of the silanol number. The silanol number is defined as follows:

$$n_{SiOH} = \frac{\text{wt \% C} \times N_A}{3 \times MM_C \times S_{BET} \times 10^{18} \times \left(100 - \frac{\text{wt \% C} \times MM_{SiC_3H_8}}{3 \times MM_C}\right)}$$

where the weight percentage of carbon (wt % C) is determined with microanalysis, N_A is the Avogadro constant, S_{BET} is the BET surface area of the concerned mesoporous sample, and MM is the molecular mass of the concerned molecule or atom (in subscript). The factor 10^{18} is due to the conversion of the BET surface area from m^2/g to nm^2/g, and the factor 3 originates from the 1 silanol being replaced by 3 carbons. The last part of the denominator takes into account the conversion from the weight percentage of carbon on the TMS-modified sample to the resulting weight percentage of hydroxyls on the sample before modification. During the modification one hydrogen is substituted for TMS resulting in a net substitution of one silicium, three carbon, and eight hydrogen atoms.

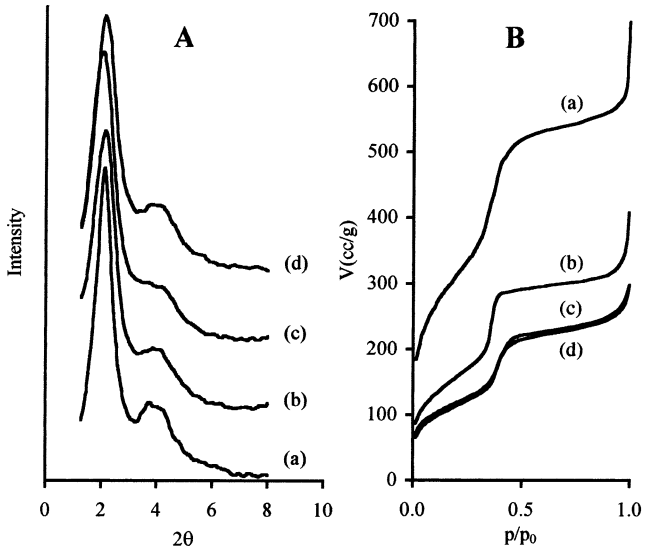

Figure 2. (A) XRD patterns and (B) N_2 isotherms of (a) FSMSap, (b) FSMSap $NaAlO_2$, (c) FSMSap $Al(NO_3)_3$, and (d) FSMSap $Al(i\text{-}C_3H_7O)_3$.

The main error in the determination of the surface silanol concentration is in both cases the standard deviation on the experimental data, which is 0.2 OH/nm.

Results and Discussion

(a) Synthesis of Al−FSMSap Materials. The mesoporous aluminosilicate FSMSap samples (Al−FSMSaps) were synthesized in the presence of different aluminum sources [$NaAlO_2$, $Al(NO_3)_3$, and $Al(i\text{-}C_3H_7O)$]. The obtained low Si/Al ratios (10.6−13.2) of the actual samples in the Na^+ form are depicted in Table 1. The samples synthesized in the presence of an aluminum source have lower Si/Al ratios than the FSMSap sample, indicating that at least a part of the aluminum is condensed into the mesoporous structure or present as another crystal (sodium aluminum silicate hydroxide hydrate crystals for instance). By analyzing the X-ray diffraction patterns and nitrogen adsorption isotherms at 77 K (Figure 2A and B, respectively), the influence of the aluminum source on the crystallinity and structural properties of the synthesized mesoporous Al−FSMSaps in the Na^+ form can be deduced. The XRD patterns of the calcined samples correspond to those usually observed for other aluminosilicate hexagonally ordered mesoporous materials (AlSi−HMM) with the same low Si/Al ratio.[4,6,8,9,11] All samples exhibit at least one well-resolved reflection of an ordered hexagonal

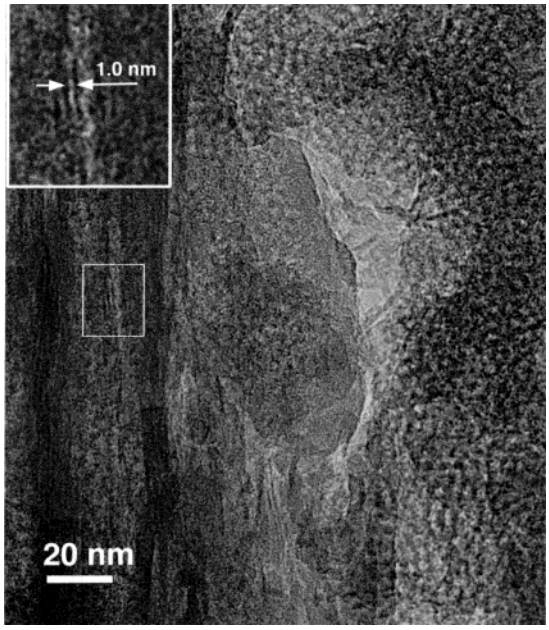

Figure 3. Transmission electron micrograph of FSMSap, and inset showing magnification of the rectangle indicating the leached clay zone.

lattice in the low angle region between 2 and 10° 2θ. In the high angle region between 15 and 30° 2θ (not shown here), a very broad diffraction peak attributed to the amorphous silica wall is appearing, beside the remaining narrow saponite bands. As no other bands emerged, this points out that no other crystalline phase is formed.[10] FSM materials with only one single peak exhibit a short-range hexagonal arrangement as shown by Chen et al.[12] The transmission electron microscopy (TEM) observation of FSMSap indeed confirmed these findings. Two phases, attributed to leached saponite and the mesoporous material, could be clearly observed in the TEM image in Figure 3. In the inset a region with layered material was magnified. The original saponite platelets are 9.6 Å high, making it highly presumable that the layers, identified in the inset with a *d* spacing of around 10 Å, are due to the leached saponite. The porous structure, synthesized from the leached saponite, could be observed at the right side of the micrograph showing a pore diameter in the range of 25−30 Å. As evidenced by a deconvolution method (not shown here) the shoulder of the basal peak is caused by diffuse higher order peaks of a hexagonally ordered material (110 and 200 reflections). However, in the case of the sample prepared with the aluminum nitrate source, the reflections of the higher order peaks are broadened as the result of a decrease in crystallinity.[7] This is probably due to the lowering of pH of the reaction mixture prepared using the aluminumnitrate source. As shown in Table 1 the unit cell parameter (a) of the four Al−FSMSaps is either 4.5, 4.6, or 5.0 nm. The unit cell parameter of the FSMSap sample is rather high for an AlSi−HMM material with a Si/Al ratio of 12.8.[8,13] The corresponding adsorption isotherm is of type IV in the BDDT (Brunauer, Deming, Deming, Teller) classification and similar in shape to the nitrogen isotherm of other aluminosilicate hexagonally ordered mesoporous materials (AlSi−HMM). All the samples have a sharp step in their adsorption isotherms reflecting the filling of the mesopores (see Figure 2B). On the basis of the nitrogen adsorption data (see Table 1), the FSMSap (synthesized without an additional aluminum source) is the most optimal sample, having a BET surface area of 1130 m^2/g and pore volume of 0.92 cm^3/g. Analyzing the corresponding nitrogen adsorption isotherm and its deduced pore size distributions (BJH method) a pore size diameter of 2.7 nm was calculated for this sample. Furthermore, the data in Table 1 confirm the poorly crystallized nature of the FSMSap $Al(NO_3)_3$ sample, in agreement with the XRD results. The reduced specific surface area and pore volume of the Al−FSMSap samples arise from two causes. First, the thermal stability of SiAl−HMMs becomes lower with a decreasing Si/Al ratio because of dealumination during the calcination based on the combination of the high local temperatures achieved during the combustion of the template, and the steam generated during the combustion of the organic in the presence of air.[4,14] Second, the formation of the FSMSaps is susceptible to the addition of the different Al sources during the synthesis, suffering an undesirable decrease in the structure ordering.[15] Apparently the Al−FSMSap sample synthesized in the presence of sodiumaluminate exhibits an ultimate low Si/Al ratio of 10.6, a pore volume of 0.98 cm^3/g, a specific surface area of 565 m^2/g, and a pore diameter of 3.0 nm, being the best retained structure synthesized with an additional aluminum source. However, the blanc FSMSap with the highest Si/Al ratio of 12.8 remains the most optimal structure in terms of surface area and porosity.

(b) Mechanical, Thermal, and Hydrothermal Stability. Anticipating the possible applications of the FSMSap materials one has to take into account the extreme conditions that could be imposed on these mesoporous materials during industrial processes. Therefore, important physical properties such as thermal, hydrothermal, and mechanical stability of the FSMSaps were investigated and compared with those of a FSM synthesized from kanemite (FSMKan). For each stability test the sample heated at the common calcination temperature of 550 °C was taken as the reference sample (see the first row of Table 2). First, the stability of the most optimal sample, FSMSap, and subsequently the effect of additional aluminum incorporation on the stability of the FSMSap sample, was investigated. Comparing the stability of the Al−FSMSap samples and the original FSMSap sample one has to be aware of the fact that the lower structure ordering of the Al−FSMSap samples will also have its repercussion on the stability.

Mechanical Stability. X-ray diffractograms of the samples subjected to pressures of 296 and 444 MPa were recorded to examine the mechanical stability. As shown in Figure 4A, the structural degradation of both FSMKan and FSMSap rendered a considerable decrease in

(11) Zhao, D.; Nie, C.; Zhou, Y.; Xia, S.; Huang, L.; Li, Q. *Catal. Today* **2001**, *68*, 11.
(12) Chen, C.-Y.; Xiao, S.-Q.; Davis, M. E. *Microporous Mater.* **1995**, *4*, 1.
(13) Koch, H.; Böhmer, U.; Klemt, A.; Reschetilowski, W.; Stöcker, M. *Faraday Discuss.* **1998**, *94*, 817.
(14) Inaki, Y.; Yoshida, H.; Kimura, K.; Inagaki, S.; Fukushima, Y.; Hattori, T. *Phys. Chem. Chem. Phys.* **2000**, *2*, 5293.
(15) Oumi, Y.; Takagi, H.; Sumiya, S.; Mizuno, R.; Uozumi, T.; Sano, T. *Microporous Mesoporous Mater.* **2001**, *44*−*45*, 267.

Table 2. Physical Properties of the Mechanical-, Thermal-, and Hydrothermal-Treated FSMSaps and FSMKan

	FSMKan		FSMSap		FSMSap $NaAlO_2$		FSMSap $Al(NO_3)_3$		FSMSap $Al(i\text{-}C_3H_7O)_3$	
treatment conditions	S_{BET} (m^2/g)	PV (cc/g)	S_{BET} (m^2/g)	PV (cc/g)	S_{BET} (m^2/g)	PV (cc/g)	S_{BET} (m^2/g)	PV (cc/g)	S_{BET} (m^2/g)	PV (cc/g)
					Thermal Stability					
550 °C	1027	0.91	1172	0.78	565	0.98	399	0.42	426	0.43
650 °C	970	0.76	1112	0.64	382	0.41	408	0.44	299	0.33
750 °C	879	0.68	915	0.44	397	0.50	376	0.37	270	0.32
850 °C	795	0.53	476	0.20	219	0.23	218	0.27	201	0.28
					Hydrothermal Stability					
300 °C, 30 vol % steam, 120 h	987	0.81	1060	0.66	336	0.36	331	0.33	239	0.31
400 °C, 30 vol % steam, 48 h	892	0.66	995	0.52	356	0.37	373	0.42	313	0.39
400 °C, 30 vol % steam, 120 h	864	0.59	789	0.36	370	0.37	336	0.38	278	0.32
100 °C, 100% relative humidity, 16 h	106		67		333	0.33	196	0.22	130	0.17
					Mechanical Stability					
296 MPa	729	0.54	532		296	0.27	280	0.26	299	0.28

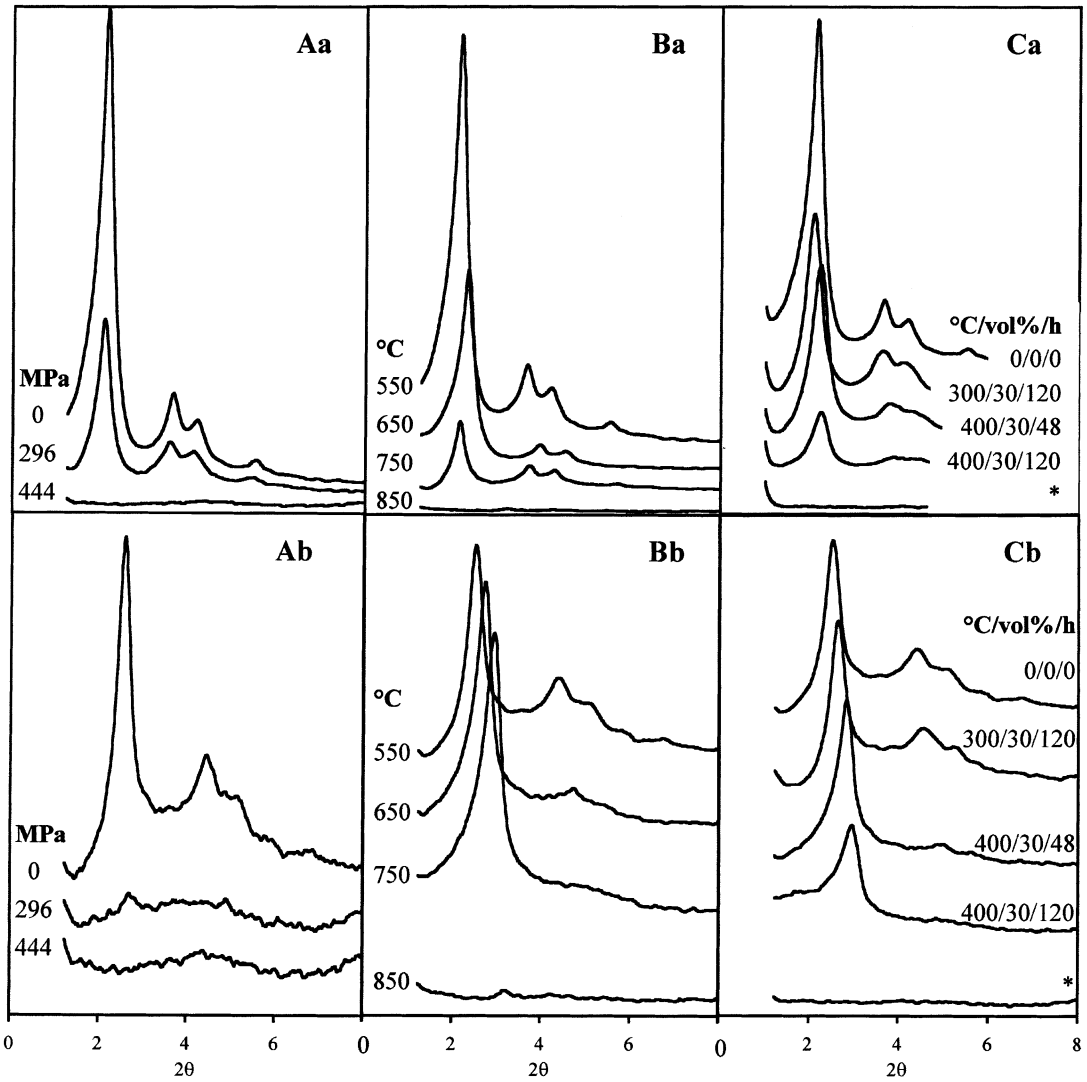

Figure 4. (A) Mechanical, (B) thermal, and (C) hydrothermal stability of (a) FSMkan and (b) FSMSap (*: 100 °C/100% relative humidity/16 h).

the XRD peak intensity of the 100 plane. At the same time, the inflection point caused by capillary condensation in the nitrogen adsorption isotherms is also less unambiguous. Apparently, as derived from the data of the nitrogen adsorption isotherm for the samples compressed to 296 MPa, summarized in Table 2, a considerable reduction of the BET surface area and pore volume was observed after performing the mechanical stability test. From the obtained data it can be deduced that the ordered mesoporosity of the HMMs is essentially lost

at pelletizing pressures of 296 and 444 MPa for, respectively, FSMSap and FSMKan. These mechanical stabilities are in accordance with previously obtained results for other hexagonal mesoporous materials.[16−19] Comparing the nitrogen adsorption data of both samples at a compression of 296 MPa, it is obvious that the FSMSap sample is less stable toward unilateral compression than the FSMKan sample. The BET surface area of FSMSap is reduced to 45% of its initial value, whereas only a 30% decrease was found for FSMKan. Similarly, a much higher pore volume decrement can be observed for FSMSap than for FSMKan. The rather low mechanical stability of aluminosilicate HMMs compared to pure silicon HMMs can be explained in terms of the different mechanisms of the structural collapse. The fragility of the FSMSap material is likely to be attributed to the partial dealumination of aluminosilicate mesoporous materials. As shown previously, the incorporated Al in the AlSi−HMM framework is unstable and can be converted to nonstructural aluminum species in the presence of water.[20] It also has been reported that the breaking of the Si−O−Si and certainly the Si−O−Al bonds by water is promoted by compression.[17] Furthermore, taking into account the hydrophilic properties caused by the negative charge of the structure, one can expect the migration of aluminum out of the framework due to the mechanical pressure imposed on the AlSi−HMMs. A similar trend can be observed for the three Al−FSMSap samples with additional incorporated aluminum, all showing a substantial decrease in specific surface area and pore volume. However, the fact that no additional loss of the mechanical stability occurred compared to the original sample is worth mentioning.

Thermal Stability. For investigating the thermal stability, the samples are calcined between 550 and 850 °C. As depicted in Figure 4B both samples have comparable X-ray diffraction patterns after an initial calcination at 550 °C for 6 h. The XRD of FSMKan and FSMSap presents a typical four-peak pattern with a high-intensity peak at a low 2θ (d(100)) and three weaker peaks at a higher 2θ (d(110), d(200), d(210)). The intensity of all peaks decreased with higher calcination temperatures until the three diffractions at higher angle disappeared at a calcination temperature of 850 °C, indicating a loss in the structure ordering. Accordingly, the BET surface area and pore volume shown in Table 2 decreased with the calcination temperature. When subjected to a calcination temperature of 850 °C, the FSMSap and the FSMKan sample, respectively, suffer 60% and 20% decreases in BET surface area. The two samples still have a small capillary condensation step in the isotherm (not shown) and a 100 reflection in the X-ray diffractogram at a calcination temperature of 750 °C, but both disappear at 850 °C as a result of a complete collapse of the framework-confined mesopores. Furthermore, the unit cell contraction for FSMSap (from 38.7 to 33.9 Å) is higher than that for FSMKan (from 46.5 to 43.4 Å) when the calcination temperature is increased from 550 to 750 °C. As shown previously,[15] this feature indicates that dealumination of the FSMSap sample occurs at higher temperatures. When comparing the thermal stability of the samples with additional Al incorporation with the two former samples, some features attract attention. Upon calcination at 750 °C, the FSMSap $Al(NO_3)_3$ and FSMSap $Al(i\text{-}C_3H_7O)_3$ samples, respectively, suffer 10 and 25% decreases in pore volume, being lower than the 45% loss for FSMSap. The stability of the FSMSap $NaAlO_2$ sample however is comparable to that of the FSMSap sample. Apparently, an additional incorporation with aluminum nitrate or aluminum triisopropoxide results in a higher thermal stability of the FSMSap sample.

Hydrothermal Stability. From a practical point of view, especially with respect to the regeneration of AlSi−HMMs in superheated steam, the hydrothermal stability is a crucial factor. Therefore, the stability of FSMSap toward steam was investigated by recording X-ray diffractograms (Figure 4C) and nitrogen adsorption isotherms. The XRD patterns reveal that FSMSap and FSMKan structurally suffer from the steaming test. Because of destruction effects, the (100) diffraction peak intensity decreases analogously for both samples, eventually disappearing after the treatment for 16 h at a relative humidity of 100%. Furthermore, the unit cell contraction, occurring for a more severe hydrothermal treatment, is higher for FSMSap (from 38.7 to 33.6 Å) than that for FSMKan (from 44.5 to 46.5 Å). The physical properties of the samples before (calcined at 550 °C) and after the hydrothermal treatments are displayed in Table 2. For FSMKan, a clear retention of the pore structure can be observed after a treatment of 30 vol % steam at 400 °C for 120 h, showing only a small relative decrease in specific surface area (15% of the initial surface area). In contrast, a significant loss in specific surface area can be observed for FSMSap (35% of the initial surface area). The most severe steaming test, exposing the samples to steam at autogenous pressure, resulted in the total collapse of the framework for both samples, reducing the surface areas to ∼100 m^2/g and converting the peak intensities of the (100) plane to zero. The mechanism of the hydrothermal breakdown of HMMs is thought to proceed via the hydrolysis of the Si−O−Si bonds.[16] As proven by Shen et al.,[20] under a mild hydrothermal treatment the incorporated Al in the AlSi−HMM framework is unstable and can be converted to nonstructural aluminum species. Therefore, one can expect structural defect sites, created by the migration of aluminum out of the framework, resulting in a lower structure ordering. Furthermore, this feature is consolidated by the more hydrophilic character of aluminosilicates, resulting in a lower steam resistance. However, upon additional incorporation of aluminum with $NaAlO_2$, $Al(NO_3)_3$, or $Al(i\text{-}C_3H_7O)_3$ the hydrothermal stability increased. Figure 5, displaying the relative surface area as a function of the degree of hydrothermal treatment, indeed indicates this. Apparently, after the treatment for 16 h at

(16) Cassiers, K.; Linssen, T.; Mathieu, M.; Benjeloun, M.; Schrijnemakers, K.; Van Der Voort, P.; Cool, P.; Vansant, E. F. *Chem. Mater.* **2002**, *14*, 2317.
(17) Galarneau, A.; Desplantier-Giscard, D.; Di Renzo, F.; Fajula, F. *Catal. Today* **2001**, *68*, 191.
(18) Ishikawa, T.; Matsuda, M.; Yasukawa, A.; Kandori, K.; Fukushima, T.; Kondo, S. *J. Chem. Soc., Faraday Trans.* **1996**, *92*, 1985.
(19) Springuel-Huet, M.-A.; Bonardet, J.-L.; Gédéon, A.; Yue, Y.; Romannikov, V. N.; Fraissard, J. *Microporous Mesoporous Mater.* **2001**, *44*−*45*, 775.
(20) Shen, S. C.; Kawi, S. *J. Phys. Chem. B.* **1999**, *103*, 8870.

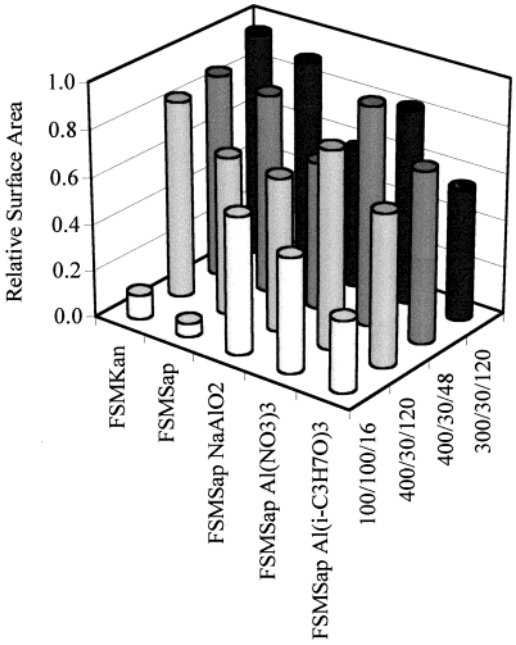

Figure 5. Relative surface area as a function of the hydrothermal test.

a relative humidity of 100%, the FSMSap $NaAlO_2$ still has a relative surface area of 60%, while the FSMSap has only 5% of its original specific surface left. The enhancement of the hydrothermal stability of AlSi−HMM by incorporation of aluminum into the framework has already been reported in previous studies.[15,21,22] As shown by Mokaya et al.,[23] a protective aluminum-rich surface layer is formed during incorporation of aluminum. It has also been reported that the hydrothermal stability can be improved by this disordered layer and the increase in thickness of the pore wall, which are caused by the presence of aluminum in the framework.[12,21] Likely, the improvement of the hydrothermal stability of HMMs by incorporation of aluminum into the framework seems to be caused here by a change in geometric and chemical properties.

(c) Study of the Cation Exchange Capacity. With their negatively charged porous framework and the small and mobile cations (Na^+) located in the pores, the AlSi−HMMs are typical ion exchangers. The aluminum, being incorporated tetragonally in the FSMSap structures, creates a cation exchange capacity (CEC). Vice versa, this implies that when the FSMSap samples have an ion exchange capacity this has to be induced by incorporated aluminum in a tetragonal coordination. In Table 1 the maximal exchange capacities (CEC_{max}) of the samples are listed, as calculated from the elemental composition of the FSMSap samples. The CEC_{max}, being about 1.1 mmol/g for the four samples, should be inversely correlated to the Si/Al ratio when all the aluminum is incorporated into the structure. Via determination of the nitrogen content of the samples by the Kjeldahl method after exchange of the mobile sodium ions with ammonium ions, the actual ion exchange capacity could be calculated (Table 1). Apparently, all the FSMSap samples have a CEC approaching the maximal cation exchange capacity. This is a very good result compared to the CEC reported before for other AlSi−HMMs.[4,24,25]

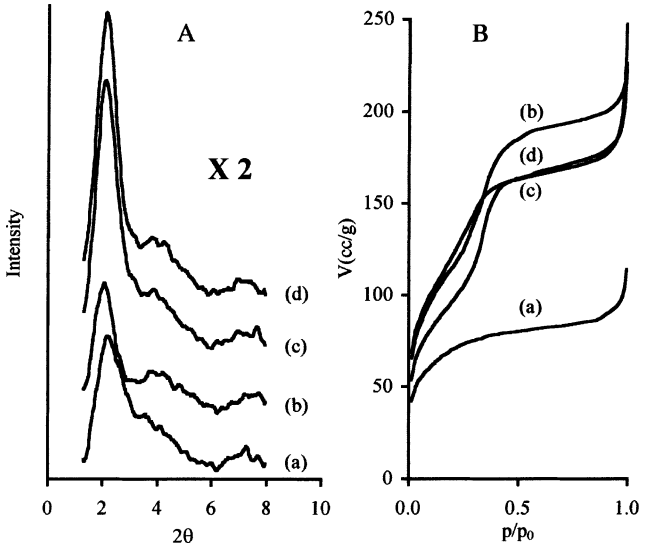

Figure 6. XRD patterns (A) and N_2 isotherms (B) of (a) FSMSap H^+, (b) FSMSap $NaAlO_2$ H^+, (c) FSMSap $Al(NO_3)_3$ H^+, and (d) FSMSap $Al(i\text{-}C_3H_7O)_3$ H^+.

When developing mesoporous catalysts, ion exchange plays an outstanding role. For many catalytic applications, a Brønsted acid form of a mesoporous aluminosilicate is required. Brønsted acid sites in AlSi−HMMs can be readily generated by introducing ammonium ions followed by a heat treatment.

The counterion in the synthesized aluminosilicate mesoporous material after synthesis is Na^+. The characterized Al−FSMSaps are converted into their acid form by extracting the Na^+ form for 6 h with a 0.5 M NH_4NO_3 solution using a liquid-to-solid ratio of 20 wt %. In comparison to the samples in the Na^+ form, the acidic Al−FSMSap materials (Al−FSMSap H^+ samples) have only slightly higher Si/Al ratios (see Table 1), indicating that a negligible amount of aluminum is dissolved in the solution during the applied acidifying procedure. Consequently, as depicted in Table 1, the unit cell dimensions of the mesoporous materials calculated from the d_{100} values in the XRD patterns, being dependent on the Si/Al ratio,[13] remained unchanged. The diffraction patterns still correspond to those of mesoporous materials with a hexagonal structure, but the peaks are less intense, pointing out a decrease in structure ordering (Figure 6A) due to the aqueous acid treatment of the FSMSap samples. In comparison to other acidified AlSi−HMM materials with the same low Si/Al ratio the peaks are well-resolved.[4,26−28] The corresponding adsorption isotherms are of type IV in the BDDT classification and similar in shape to the nitrogen isotherm of a common HMM (Figure 6B). On the other

(21) Ryoo, R.; Kim, J. M., Ko, C. H.; Shin, D. H. *J. Phys. Chem.* **1996**, *100*, 17718.
(22) Mokaya, R. *Chem. Commun.* **2001**, *10*, 933.
(23) Mokaya, R. *J. Catal.* **1999**, *186*, 186.
(24) Kosslick, H.; Lischke, G.; Parlitz, B.; Storek, W.; Fricke, R. *Appl. Catal.* **1999**, *184*, 49.
(25) Reddy, K. M.; Song, C. *Catal. Lett.* **1996**, *36*, 103.
(26) Wan, Y.; Wang, Z.; Ma, J. X.; Jin, X. M.; Zhou, W. *Acta Chim. Sinica* **2002**, *60*, 71.
(27) Chatterjee, M.; Iwasaki, T.; Hayashi, H.; Onodera, Y.; Ebina, T.; Nagase, T. *Catal. Lett.* **1998**, *52*, 21
(28) Liepold, A.; Roos, K.; Reschetilowski, W.; Esculcas, A. P.; Rocha, J.; Philippou, A.; Anderson, M. W. *J. Chem. Soc., Faraday Trans.* **1996**, *92*, 4623.

hand, on the basis of the nitrogen adsorption results, a decrease in the BET surface areas of 75% for FSMSap and only 25% for the Al−FSMSaps is observed after the acidifying procedure. Several articles already discussed the stability of mesoporous materials in aqueous media.[29−31] As a result of silicate hydrolysis of the relatively thin silica walls, the Si−HMMs are less stable in contact with water than the AlSi−HMMs. Because of this feature, aluminosilicate materials with a low Si/Al have a significantly higher stability toward suspension in water. This feature accounts for the higher stability toward the acidifying step of the Al−FSMSaps (Si/Al ≈ 11) synthesized with an additional aluminum source in comparison with the FSMSap (Si/Al ≈ 13). To conclude, from a structural point of view, one can say that the Al−FSMSap H^+ samples with a high aluminum content (Si/Al ∼11), synthesized with an additional aluminum source, all have a high unit cell parameter (± 4.8 nm), surface area (± 400 m^2/g), and pore volume (± 0.3 cm^3/g), and a fairly narrow pore size distribution (± 3 nm). In agreement with the results obtained by Corma et al.,[4] sodium aluminate is probably the best aluminum source to prepare HMM samples with low Si/Al, showing slightly better structural properties.

(d) Determination of the Aluminum Coordination. The ^{27}Al NMR spectra are potentially very helpful for probing the quantity, coordination, and location of aluminum atoms in aluminosilicates, since X-ray diffraction only elucidates the long-range order of these materials. Nevertheless, the quadrupolar nature of the nucleus does not allow the observation of the structurally significant fine structure of the bands, limiting the applicability of ^{27}Al MAS NMR to little more than the determination of the coordination number at the aluminum atom.

Bearing in mind that the final synthesized and acidified material consists of the Al−FSMSap H^+ sample and a residual fraction of leached Saponite, the NMR spectra in Figure 7 are clarified, and the peaks are listed in Table 3. As determined from existing literature, the natural Saponite (from Ballarat, CA) shows only one ^{27}Al peak centered at 67 ppm (not shown), in the region corresponding to tetrahedrally coordinated aluminum (Al^{IV}), confirming the absence of aluminum atoms in the octahedral sheet.[32,33] The ^{27}Al NMR spectra of the Al−FSMSap H^+ samples are clearly dominated by the signal in the range around 60 ppm, which is characteristic of tetrahedrally coordinated (framework) Al sites. The small resonances on either side of the principal resonance, indicated in Figure 7 with an asterisk, are spinning sidebands, which are due to partial averaging of the quadrupolar interactions.[34] Exact positions and relative areas of the spectral components were calculated by spectral deconvolution. The signals at 67 and 53 ppm are both due to tetrahedrally coordinated aluminum, respectively present in the residual Saponite and the mesoporous aluminosilicate (in which aluminum is covalently bound to four Si atoms via oxygen bridges). As already mentioned in a previous section, the aluminum, being incorporated tetragonally in the FSMSap structures, creates a cation exchange capacity (CEC). Therefore, the high content of tetrahedral aluminum, reaching values up to 85% of the total aluminum content, accounts for the high CEC values obtained for the Al−FSMSap samples. Indeed the CEC of the Al−FSMSap samples reaches up to 90% of the maximal CEC value that is calculated as if all the aluminum

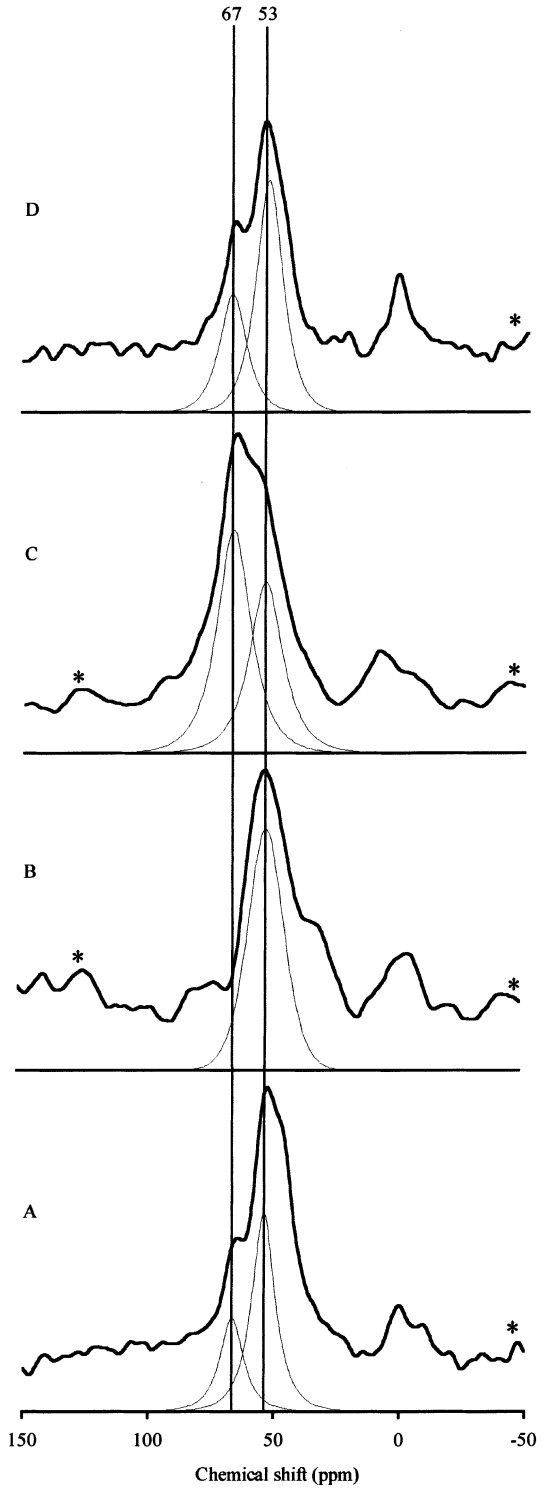

Figure 7. ^{27}Al MAS NMR spectra and deconvolution on the principal two peaks around 60 ppm of (A) FSMSap H^+, (B) FSMSap $NaAlO_2$ H^+, (C) FSMSap $Al(NO_3)_3$ H^+, and (D) FSMSap $Al(i\text{-}C_3H_7O)_3$ H^+.

(29) Chen, L. Y.; Jaenicke, S.; Chuah, G. K. *Microporous Mater.* **1997**, *12*, 323.
(30) Shen, S.-C.; Kawi, S. *J. Phys. Chem. B* **1999**, *103*, 8870.
(31) Mokaya, R. *J. Phys. Chem. B* **2000**, *104*, 8279.
(32) Storaro, L.; Lenarda, M.; Perissinotto, M.; Lucchini, V.; Ganzerla, R. *Microporous Mesoporous Mater.* **1998**, *20*, 317.
(33) Woessner, D. E. *Am. Mineral.* **1989**, *74*, 203.
(34) Fyfe, C. A.; Thomas, J. M.; Klinowski, J.; Gobbi, G. C. *Angew. Chem., Int. Ed. Engl.* **1983**, *22*, 259.

Table 3. Results of the Deconvolution of ^{27}Al MAS NMR Spectra of the Al−FSMSap H$^+$: Relative Portions (%) of Different Coordinated Al Sites

type	FSMSap H$^+$	FSMSap $NaAlO_2$ H$^+$	FSMSap $Al(NO_3)_3$ H$^+$	FSMSap Al(*i*-$C_3H_7O)_3$ H$^+$
		Al^{IV} Coordination		
clay	17	0	49	28
FSM	37	63	36	54
distorted	30	20	0	0
total	84	83	85	82
		Al^{VI} Coordination		
	16	17	15	18

would be incorporated in the samples as tetrahedral aluminum. This high CEC value apparently originates from two types of tetrahedral aluminum present in the residual Saponite and the mesoporous aluminosilicate. Mean values of deconvolution data obtained by several different fitting strategies show that, for the original FSMSap H$^+$ and the FSMSap Al(*i*-$C_3H_7O)_3$ H$^+$ sample, $^1/_3$ of the Al^{IV} originates from the leached clay, while $^2/_3$ is incorporated into tetrahedral framework positions of the mesoporous sample. The FSMSap $NaAlO_2$ H$^+$ sample showed no peak at 67 ppm, pointing out that almost all the tetrahedral aluminum is derived from the incorporation of the aluminum into tetrahedral framework positions of the mesoporous structure. In the FSMSap $Al(NO_3)_3$ H$^+$ sample, however, about 60% of the Al^{IV} originates from the Saponite while only 40% is incorporated into the mesoporous structure. The presence of a residual leached clay fraction was already observed by XRD analysis at high angles 2θ and IR measurements and is now confirmed by Al^{27}-NMR. The spectra of the FSMSap H$^+$ and the FSMSap $NaAlO_2$ H$^+$ samples showed, in addition to the peaks attributed to tetrahedral and octahedral aluminum, additional shoulders at different chemical shift values. According to various authors[32,35,36] these peaks can be attributed to aluminum in a highly distorted tetrahedral coordination. In all cases, also the presence of octahedrally coordinated (nonframework) aluminum is indicated by the comparably weak signal in the region around 0 ppm. The broad asymmetric Al^{VI} NMR peak indicates multiple octahedral-site environments, being sensitive to different substitutions.[37] The respective relative peak intensities are calculated by spectral deconvolution and listed in Table 3. Assuming that the concentrations of the tetrahedral and octahedral aluminum are proportional to the respective intensities of the resonances in the range around 60 and 0 ppm, it is observed that the ratio of aluminum in the tetrahedral to that of aluminum in the octahedral environment (Al^{IV}/Al^{VI}) increases in the order of FSMSap Al(*i*-$C_3H_7O)_3$ H$^+$ < FSMSap $NaAlO_2$ H$^+$ < FSMSap H$^+$ < FSMSap $Al(NO_3)_3$ H$^+$. The relative peak intensities, as calculated in Table 3, further verify that $AlNO_3$ is superior to the other aluminum sources in providing higher concentrations of tetrahedral aluminum for FSMSap aluminum incorporation.

(e) Determination of Surface Silanol Concentration. Knowledge of the exact concentration of silanols on the surface of the mesoporous materials is required in order to predict the maximal number of catalytic sites that can be deposited onto the surface by reaction of the silanols with a suitable catalyst precursor molecule. Already many articles report on the modification via the anchoring of different functional groups on HMM samples for advanced applications, e.g., in catalysis,[38] and selective adsorption of organics[39] and metals.[40] Previously the silanol number of mesoporous silicates was already determined in different ways by theoretical calculations,[41] chemical methods,[42] and physical methods.[43] As an overall conclusion one can say that all the hexagonal mesoporous materials possess a high hydrophobicity in comparison with silica gels ($n_{SiOH} = 5-6$), the FSMKan having around 3 OH/nm^2. In this study, the quantification of the SiOH number was performed via a new chemical modification technique, being the reaction with trimethylchlorosilane (TMSCl). In case of the determination of the hydrophobicity of silica gels, not all the silanols react with the TMSCl because of the voluminous transition state in the liquid phase, where both the catalyst (triethylamine) and the chlorosilane must reach the surface silanol to get any reaction.[44] As proven by Kimura et al.,[45] due to the relatively low amount of SiOHs, almost all the isolated silanols of hexagonal mesoporous materials react with TMSCl. Therefore, taking two former articles into consideration, it is clear that this technique is very appropriate for the quantification of the silanols on the surface. The fundamentals of this method are based on the reaction of the isolated surface silanols with TMSCl in the presence of a catalyst (triethylamine) in a 1:1 ratio. Taking a closer look at the reaction mechanism, it is clear that one silanol group is replaced by three methyl groups. Recording a TGA of the silylated material, the oxidation and the consequent weight loss of the organic material are obtained. As depicted in the inset of Figure 8, the TGA of the silylated FSMSap shows two main weight losses at 170 and 500 °C. To gain insight into the process, an in situ DRIFT of the silylated FSMSap was taken as a function of the temperature. The progressive variation of the bands as a function of the temperature can be

(35) Chaudhari, K.; Das, T. K.; Chandwadkar, A. J.; Sivasanker, S. *J. Catal.* **1999**, *186*, 81.
(36) Lambert, J. F.; Millman, W. S.; Fripiat, J. J. *J. Am. Chem. Soc.* **1989**, *133*, 263.
(37) Woessner, D. E. *Am. Mineral.* **1989**, *74*, 203.
(38) Ying, J. Y.; Mehnert, C. P.; Wong, M. S. *Angew. Chem., Int. Ed.* **1999**, *38*, 56.
(39) Zhao, X. S.; Lu, G. Q.; Hu, X. *Microporous Mesoporous Mater.* **2000**, *41*, 37.
(40) Mercier, L.; Pinnavaia, T. J. *Adv. Mater.* **1997**, *9*, 500.
(41) Alami, E.; Beinert, G.; Marie, P.; Zana, R. *Langmuir* **1993**, *9*, 1465.
(42) Benjelloun, M.; Cool, P.; Van Der Voort, P.; Vansant, E. F. *Phys. Chem. Chem. Phys.* **2002**, *4*, 2818.
(43) Ishikawa, T.; Matsuda, M.; Yasukawa, A.; Kandori, K.; Inagaki, S.; Fukushima, T.; Kondo, S. *J. Chem. Soc., Faraday Trans.* **1996**, *92*, 1985.
(44) Impens, N. R. E. N.; van der Voort, P.; Vansant, E. F. *Microporous Mesoporous Mater.* **1999**, *28*, 217.
(45) Kimura, T.; Saeki, S.; Sugahara, Y.; Kuroda, K. *Langmuir* **1999**, *15*, 2794.

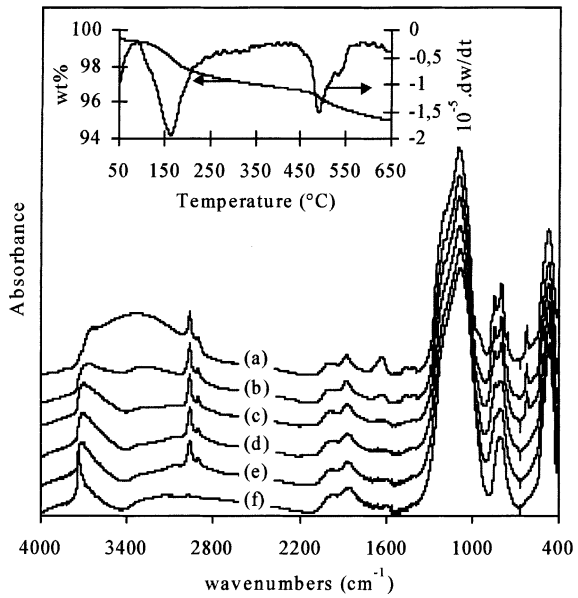

Figure 8. Determination of n_{SiOH} of FSMSap with TGA (inset) and in situ DRIFT at different temperatures ranging from 25 °C (a), over 100 °C (b), 200 °C (c), 300 °C (d), 400 °C (e), and to 500 °C (f).

observed in Figure 8. Changes in the stretching vibration mode of the hydroxyl groups and in the water molecules bonded to the different metallic cations are observed in the region between 4000 and 3000 cm^{-1}. The two weaker bands at 2000 and 1870 cm^{-1} remain at higher temperatures and are assigned to combination and/or overtones of lattice modes, while the band at 1630 cm^{-1} is attributed to the bending vibration of adsorbed water molecules. As already claimed, all the isolated silanols reacted with TMSCl, resulting in the absence of the band at 3740 cm^{-1} for spectrum a. During the thermal treatment, the band at 3740 cm^{-1} appears at 500 °C (spectrum f), pointing out the release of the isolated silanols by oxidation of the organics. This hypothesis is confirmed when considering the bands between 3000 and 2900 cm^{-1} corresponding to the methyl groups. However, alternatively to the mechanism proposed previously, it could also be the triethylamine that is strongly adsorbed on the surface. The IR spectrum with the broad feature between 4000 and 3000 cm^{-1} may in fact suggest this. This band could be due to adsorbed water, as previously assumed, but also could be due to the amine interacting with OH groups. Examining the nitrogen content of the H^+ form of FSMSaps with the Perkin-Elmer CHN analyzer we found that no nitrogen is present in either of the samples after they were thoroughly washed with CH_2Cl_2. Therefore, one can conclude that the mass loss is exclusively due to the combustion of the methyl groups of the TMS, and the quantification of the silanols should be calculated from the second weight loss at 500 °C. Taking into account former findings, the SiOH numbers were estimated to be 0.8 and 2.7 for the acidified forms of FSMSap and FSMKan, respectively, in accordance with the preceding literature. As a reference method, carbon analysis was performed on the samples treated with TMSCl. Relative weights of 4.6% and 11.8% carbon were found for the H^+ forms of FSMSap and FSMKan, respectively, corresponding to SiOH numbers of 0.9 and 2.9. These results are in good agreement with those obtained from the TGA data. The silanol numbers of the other samples were determined similarly and are reported in the last column of Table 1. The significantly lower silanol number of the FSMSap is probably due to the lower surface area of this sample compared to that of FSMKan.

Conclusion

The influence of an additional Al incorporation, utilizing different aluminum sources, on the structure of Na^+−FSMSap was studied. It is shown that mesoporous aluminosilicates derived from saponite can be synthesized with a high porosity (surface area of 1130 m^2/g and pore volume of 0.92 cm^3/g) having a low Si/Al ratio of 12.8 and high mechanical, thermal, and hydrothermal stability. They have a remarkable cation exchange capacity of around 1 mmol/g and a high silanol number of about 0.7 OH/nm^2, both characteristics being interesting for high-yield postsynthesis modification reactions. Exchange with ammonium ions and a consecutive heat treatment transformed the aluminosilicates into their Brønsted acid form generating acidic properties.

A thorough investigation was performed on the physical and chemical characteristics of this promising aluminosilicate FSMSap. Incorporation with $Al(NO_3)_3$ or $Al(i\text{-}C_3H_7O)_3$ increased the mechanical stability (70% of the specific surface area was retained at a unilateral pressure of 296 Mpa) up to the same stability as FSM synthesized from kanemite. Additional incorporation with these aluminum sources also resulted in a higher thermal stability of the FSMSap sample (the relative pore volume of the FSM $Al(NO_3)_3$ sample still was 90% after a calcination temperature of 750 °C). The hydrothermal stability under severe conditions (relative humidity of 100% for 16 h) of the FSMSap sample was improved upon incorporation of aluminum retaining now up to 60% of the surface area when using $NaAlO_2$ as additional aluminum source, compared to only 5% in the absence of an aluminum source.

Apparently, all the FSMSap samples have an extremely high cation exchange capacity (1 mmol/g) in comparison with the CEC of other AlSi−HMMs reported in the literature. This high CEC value originates from the high content of tetrahedral aluminum (85%) in the FSMSap samples. The silanol number was determined from the weight loss in the TGA after reaction with TMSCl and estimated to be 0.9 OHs/nm^2, a number which is confirmed by CHN analysis.

The presence of a residual leached clay fraction was also confirmed by Al^{27} NMR. According to ^{27}Al NMR studies, $AlNO_3$ is superior to the other aluminum sources in providing higher concentrations of tetrahedral aluminum for FSMSap aluminum incorporation.

Brønsted acid sites in the FSMSaps were readily generated by introducing ammonium ions into the structures, followed by a heat treatment. Because of the negligible amount of aluminum being dissolved in the solution during the applied acidifying procedure, the XRD peaks were well-resolved in comparison to those of other acidified AlSi−HMM materials reported in the literature with the same low Si/Al ratio.

To conclude, from a structural point of view, one can say that the Al−FSMSap samples in the H^+ form with a high aluminum content (Si/Al ∼11), synthesized with

an additional aluminum source, all have a high unit cell parameter (±4.8 nm), surface area (±400 m^2/g), and pore volume (±0.3 cm^3/g), and a fairly narrow pore size distribution (±3 nm). In agreement with the results obtained in the literature, sodium aluminate is probably the best aluminum source to prepare HMM samples with low Si/Al, showing slightly better structural properties.

Acknowledgment. T.L. is indebted to the IWT for financial support. P.C. acknowledges the FWO Vlaanderen (Fund for Scientific Research, Flanders, Belgium) for financial support. O.L. performed this work within the framework of IUAP 4/10. The authors gratefully thank N. Calluy for performing the CHN analyses.

CM031111A